

Table I. Frequency Assignments^a for Solid K₂M(CN)₄

		M		
		Zn	Cd	Hg
A _{1g}	ν _{1a} (r _{CN})	2154.8 ± 0.2	2146.4 ± 0.2	2149.1 ± 0.2
	ν _{2a} (r _{MC})	340.5 ± 0.5	322.7 ± 0.5	336.9 ± 0.5
E _g	ν _{3a} (δ _{MCN})	315.9 ± 1.0	255.7 ± 0.5	275.4 ± 0.5
	ν _{4a} (δ _{CMC})	126.4 ± 0.5	114.3 ± 0.5	116.4 ± 0.5
F _{2g}	ν _{5a} (r _{CN})	2153.2 ± 0.2	2145.9 ± 0.2	2145.9 ± 0.2
	ν _{6a} (r _{MC})	348.4 ± 1.0	318.0 ± 2.0	326.9 ± 1.0
	ν _{7a} (δ _{MCN})	316 ± 2	254.5 ± 1.0	237.6 ± 1.0
	ν _{8a} (δ _{CMC})	152.5 ± 1.0	137.8 ± 1.0	130.6 ± 1.0
	ν ₁₂ (T)	59.4 ± 0.2	45.9 ± 0.2	35.0 ± 0.2
F _{1g}	ν _{9a} (δ _{MCN})	(230) ^b	(194) ^b	(180) ^b
	ν ₁₀ (rot.)			
A _{2u}	ν _{1b} (r _{CN})			
	ν _{2b} (r _{MC})			
E _u	ν _{3b} (δ _{MCN})			
	ν _{4b} (δ _{CMC})			
	ν ₁₄ (T)			
F _{1u}	ν _{5b} (r _{CN})	2152.9 ± 0.2	2145.5 ± 0.2	2145.8 ± 0.2
	ν _{6b} (r _{MC})	355.7 ± 1.0	321 ± 1	330 ± 2
	ν _{7b} (δ _{MCN})	314.4 ± 1.0	249 ± 1	232 ± 2
	ν _{8b} (δ _{CMC})	150 ± 2 }	133 ^c	140 ± 10
	ν ₁₅ (T)	126 ± 2 }		117 ± 2
	ν ₁₆ (T)	84?	71 ± 2	69 ± 2?
F _{1u}	ν _{1a} + ν _{5b} }	4281.0 ± 0.5	4267.5 ± 0.5	4268.8 ± 0.5
	ν _{5a} + ν _{5b} }			
F _{2u}	ν _{9b} (δ _{MCN})			
	ν ₁₁ (rot.)			
	ν ₁₇ (T)			

^a Units are cm⁻¹. ^b From ref 2 as estimated from combination bands. ^c This band was observed to split into two, at 147 and 124 cm⁻¹, when cooled to ~100° K.

Table II. Frequency Assignments (cm⁻¹) for Aqueous M(CN)₄²⁻

		M		
		Zn	Cd	Hg
A _{1g}	ν ₁	2151.2 ± 0.5	2144.0 ± 0.5	2147.3 ± 0.5
	ν ₂	341 ± 2	322 ± 1	334.2 ± 1
E _g	ν ₃	317 ± 1	260 ± 2	280 ± 2
	ν ₅	2149.2 ± 0.5	2142.0 ± 0.5	2143.0 ± 0.5
F ₂	ν ₇	317 ± 1	260 ± 2	232 ± 2

are A_{1g} modes at 2149 and 337 cm⁻¹ active only in A and there are F_{2g} modes at 2146 and 327 cm⁻¹ active in A and B. In Figure 2 the C orientation which should be active for only E_g modes shows that the strong peak at 166 cm⁻¹ is an E_g mode. It follows that the weak peak at 131 cm⁻¹ is F_{2g}. Residuals of strong peaks remain in "forbidden" orientations because of imperfections and misorientation. In a similar manner a weak and broad E_g mode was found at 275 cm⁻¹, a weak and broad F_{2g} mode at 238 cm⁻¹, and a fairly strong and sharp F_{2g} mode at 35 cm⁻¹.

Infrared frequencies were observed in mineral oil mulls of the powders. Aqueous Raman frequencies are presented also for comparison. The results for all three compounds are presented in Tables I and II.

There are several points of interest. As noted by Adams and Christopher for K₂Zn(CN)₄, except for the translatory lattice modes the F_{2g}-F_{1u} correlation field splitting is quite small. The low-frequency F_{2g} mode shows an unexpectedly large decrease in the series Zn-Cd-Hg. The motion involved is primarily a translation of the complex ions against the potassium atoms, which do not move. One would expect the frequency to be proportional to $m^{-1/2}$ where m is the total mass of the M(CN)₄²⁻ group. This would lead to a decrease from 59 to 52 to 44 cm⁻¹ for Zn → Cd → Hg. The significantly greater decrease observed suggests that the N-K force constant decreases in the same order [$F_{NK}(Zn) > F_{NK}(Cd) > F_{NK}(Hg)$]. Though we do not know the NK

distance for these three compounds, we would expect them to be about the same. However, it is possible that the effective charge on the nitrogen atoms varies with the metal atom causing changes in the N-K interaction. Another possibility is that variation of coupling of ν₁₂ with the other F_{2g} coordinates leads to the discrepancy. It is unfortunate that we have been unable to observe the low-frequency F_{1u} lattice mode. It would be interesting to know if it follows a similar trend.

From the correlation table we expect the inactive A_{2u} modes, ν_{1b} and ν_{2b}, to have about the same frequencies as the A_{1g} modes. The E_u modes ν_{3b} and ν_{4b} may be shifted significantly from the corresponding E_g modes by coupling the E_u translatory coordinate. We can say nothing about the F_{2u} and F_{1g} modes except for the previous assignment of ν_{9a} from combination bands,² as verified by Adams and Christopher¹ for K₂Zn(CN)₄.

We plan to observe isotope shifts for the completely substituted ¹³C and ¹⁵N species in order to estimate the force fields of these crystals. The result should help to explain the trends observed in the present work.

In order to estimate anharmonic corrections for the CN stretching modes the combinations ν_{1a} + ν_{5b} and ν_{5a} + ν_{5b} were searched for in single crystals on the Cary 14 spectrometer. For each species only one band was observed in this region (see Table I). From the nickel carbonyl spectrum⁴ one expects comparable intensities for these two combination transitions. Perhaps this is an example of the loss of intensity of one band in a Fermi resonance doublet as discussed by El Sayed.⁵ The calculated anharmonicity correction is either X_{1a,5b} or X_{5a,5b} ≈ 25 cm⁻¹ and must be viewed with some uncertainty in light of the possibility of Fermi resonance.⁵

Acknowledgment. This work was performed under the auspices of the U. S. Atomic Energy Commission.

Registry No. K₂Zn(CN)₄, 14244-62-3; K₂Cd(CN)₄, 14402-75-6; K₂Hg(CN)₄, 591-89-9.

(4) L. H. Jones, *J. Chem. Phys.*, **28**, 1215 (1958).

(5) M. El Sayed, *J. Chem. Phys.*, **37**, 680 (1962).

Contribution from the Department of Chemistry, Carnegie-Mellon University, Pittsburgh, Pennsylvania 15213

Stereochemistry of β-Diketone Complexes of Cobalt(III). XIII. Linkage and Geometrical Isomers of Thiocyanatopyridinebis(acetylacetonato)cobalt(III)

L. J. Boucher,* D. R. Herrington, and C. G. Coe

Received February 27, 1974

AIC40137C

The stereochemistry of several complexes of the type [Co(acac)₂(X)py] (X⁻ = CN⁻, N₃⁻, NCO⁻, NO₂⁻) has been studied and the marked influence of the monodentate anion on the reactivity of the complexes noted.¹ As an extension of that work we have examined the complexes of the anion NCS⁻. We wish to report here the synthesis and characterization of several isomers of the new compound [Co(acac)₂(NCS)py].²

(1) D. R. Herrington and L. J. Boucher, *Inorg. Chem.*, **12**, 2378 (1973).

(2) Abbreviations used in this paper: acac⁻, 2,4-pentanedionato (acetylacetonato); py, pyridine; DMSO, dimethyl sulfoxide.

Experimental Section

Synthesis of Complexes. $[\text{Co}_2(\text{acac})_4(\text{OH})_2]$ was prepared as previously described.³ All other materials were reagent grade and used without further purification.

***trans*-[Co(acac)₂(SCN)py].** One-half gram of $[\text{Co}_2(\text{acac})_4(\text{OH})_2]$ (0.0009 mol) was dissolved in 20 ml of cold anhydrous methanol. The solution was treated with 0.18 g of KSCN (0.0018 mol), 1.5 ml of pyridine (0.0018 mol), and then 0.10 ml of glacial acetic acid. The resulting mixture was maintained at 0° in an ice bath and stirred for 2 hr. A gold-brown solid, 0.22 g, was then isolated on a filter. The crude precipitate was washed three times with 1-ml portions of cold methanol. The complex was recrystallized by dissolution in 5 ml of chloroform and immediately adding 10-fold excess of petroleum ether (bp 30–60°). The pure solid was isolated on a filter, washed with petroleum ether, and air-dried. The yield, 0.20 g, was 28% based on the cobalt(III) used. *Anal.* Calcd for $\text{C}_{16}\text{H}_{19}\text{O}_4\text{N}_2\text{SCo}$ [Co(acac)₂(SCN)py]: C, 48.73; H, 4.82; N, 7.10. Found: C, 48.78; H, 4.89; N, 7.19. Mp 162°; *R_f* 0.68.

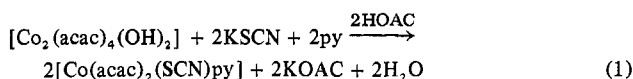
***trans*-[Co(acac)₂(NCS)py].** Two-tenths of a gram of *trans*-[Co(acac)₂(SCN)py] was dissolved in 25 ml of chloroform and the filtered solution was allowed to stand at 30° in a stoppered flask for 30 hr. The brown solid that formed was collected on a filter, washed with 5 ml of chloroform (two times), and air-dried. The yield, 0.10 g, was 50% based on the amount of Co(III) used. *Anal.* Calcd for $\text{C}_{16}\text{H}_{19}\text{O}_4\text{N}_2\text{SCo}$: C, 48.73; H, 4.82; N, 7.10. Found: C, 48.76; H, 4.90; N, 7.01. Mp 171°; *R_f*? (not sufficiently soluble).

***cis*-[Co(acac)₂(NCS)py].** A slurry of 0.10 g of *trans*-[Co(acac)₂(SCN)py] was refluxed in 50 ml of chloroform for 3 hr. The resulting solution was filtered and the filtrate concentrated to a volume of 5 ml. The solution was deposited on a chromatography column (2.5 × 30 cm) packed with 60–100 mesh Florisil (Floridin Co.). Elution with 5% methanol-benzene yielded one concentrated band. The fraction was collected, filtered, and evaporated to dryness in an airstream. Recrystallization of the residue from 5 ml of chloroform was accomplished by adding a 100-fold excess of petroleum ether. The green-brown solid was collected on a filter and air-dried. The yield, 0.05 g, was 50% based on the amount of Co(III) used. *Anal.* Calcd for $\text{C}_{16}\text{H}_{19}\text{O}_4\text{N}_2\text{SCo}$: C, 48.73; H, 4.82; N, 7.10. Found: C, 48.76; H, 4.78; N, 6.95. Mp 160°; *R_f* 0.73.

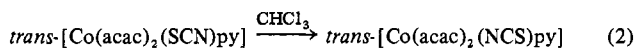
Spectral Measurements. Ultraviolet and visible spectra were obtained with a Cary 14 recording spectrophotometer. Visible spectra of the solids were taken with filter paper impregnated with a Nujol mull of the complex. A Nujol-impregnated filter paper was placed in the reference beam. Infrared spectra were taken with a Perkin-Elmer 232 spectrophotometer in the 4000–300-cm⁻¹ range with the materials in potassium bromide disks. Nuclear magnetic resonance spectra were obtained at ambient temperature with a Hitachi Perkin-Elmer Model R-20 60-MHz spectrometer. *R_f* values were determined by one development (15 cm) on 50 μ thick silica gel G plates (Analtech) with 25% methanol-benzene elution.

Results and Discussion

Synthesis. The preparation of the SCN⁻ complexes was attempted using the method previously devised for the azide complexes,⁵ *i.e.*, peroxidic oxidation of [Co(acac)₂] in the presence of various amounts of pyridine and KSCN. Unfortunately, the reaction yielded a host of products which were difficult to separate. Some of the products probably evolved from the oxidation of SCN⁻ and also from the formation of Co^{II}-NCS⁻ complexes. The charcoal-catalyzed reaction of [Co(acac)₃]⁶ with pyridine and KSCN also yielded a largely intractable mixture and the only pure product isolated was *trans*-[Co(acac)₂(py)₂]SCN. In this case, it is likely that the desired complexes underwent a charcoal-catalyzed reaction to form the most stable complex in the system. The new synthetic procedure developed here is summarized in the reaction



The reaction is carried out in a minimum of cold methanol to encourage the precipitation of the desired product. If larger amounts of solvent, or aqueous methanol or higher temperatures are used, very little product is isolated. The reaction sequence envisioned in the formation of the product starts with the acid-catalyzed splitting of the μ-hydroxo dimer with subsequent anation⁷ and pyridine-water exchange. The kinetic product in this case is the S-bonded thiocyanate trans complex (*vide infra*). When the S-bonded isomer is dissolved in chloroform and allowed to sit at room temperature linkage isomerization is noted.



Precipitation of the sparingly soluble N-bonded isothiocyanate complex (*vide infra*) is easily noted after several hours and the *t*_{1/2} for the reaction is ~4 hr at room temperature. The mixture after the reaction contains ~50% *cis*-[Co(acac)₂(NCS)py] in addition to the 50% *trans*-[Co(acac)₂(NCS)py]. Whether the *cis* forms during the intramolecular linkage isomerization or in a subsequent intramolecular geometrical isomerization is not known. Linkage isomerization is also noted in the solid state at 68°; *t*_{1/2} ≈ 12 hr. The solid-state linkage isomerization is subsequently followed by geometrical isomerization; *t*_{1/2} ≈ 2 days. The linkage isomerism of thiocyanatobis(dimethylglyoximate)(*tert*-butylpyridine)-cobalt(III) has been shown to be catalyzed by trace amounts of Co(II).^{8,9} Presumably the linkage isomerism noted here for chloroform and DMSO solutions may be subject to the same catalytic pathway. Addition of trace amounts of the oxidizing agent BrCCl₃¹⁰ to the chloroform solutions of [Co(acac)₂(SCN)py] decreased the already slow isomerization rate by about 20%.

Solutions of the thiocyanate isomer in dimethyl sulfoxide do not exclusively show linkage isomerism since the sparingly soluble isothiocyanate isomer slowly precipitates from the solution (*t*_{1/2} ≈ 48 hr at room temperature). In addition, pmr measurements of these solutions show the formation (*t*_{1/2} ≈ 5 hr at room temperature) of a species which shows three methyl resonances at -2.30, -2.25, and -2.18 ppm (intensity ratio 3:3:6) and two methine resonances at -5.62 and -5.53 ppm (intensity ratio 1:1). The addition of excess pyridine does not effect the formation of this complex, nor does the ir spectrum of the DMSO solution show any ionic SCN⁻ absorption at 2050 cm⁻¹. Since the pmr chemical shifts do not correspond to those of *cis*-[Co(acac)₂(NCS)py], it is reasonable to assume that the species formed in the pmr tube is *cis*-[Co(acac)₂(SCN)py]. The presence of small amounts of BrCCl₃ in the DMSO solution completely inhibits the slow Co(II)-catalyzed linkage isomerization of *trans*-[Co(acac)₂(SCN)py] since no precipitation of *trans*-[Co(acac)₂(NCS)py] is noted after 1 week at room temperature. On the other hand, the presence of the oxidizing agent does not effect the geometrical isomerization to *cis*-[Co(acac)₂(SCN)py].

The presence of excess SCN⁻ in the DMSO solution of

(3) L. J. Boucher and D. R. Herrington, *J. Inorg. Nucl. Chem.*, **33**, 4351 (1971).

(4) Elemental analysis by Chemalktics, Tempe, Ariz.

(5) L. J. Boucher and D. R. Herrington, *Inorg. Chem.*, **11**, 1772 (1972).

(6) H. Nishikawa, K. Konya, and M. Shibata, *Bull. Chem. Soc. Jap.*, **41**, 1492 (1968).

(7) D. A. Buckingham, I. I. Creaser, W. Marty, and A. M. Sargeson, *Inorg. Chem.*, **11**, 2738 (1972).

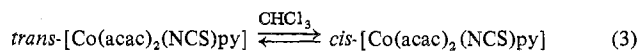
(8) R. L. Hassel and J. L. Burmeister, *Chem. Commun.*, 568 (1971).

(9) L. A. Epps and L. G. Marzilli, *J. Chem. Soc., Chem. Commun.*, 109 (1972).

(10) L. G. Marzilli, J. G. Salerno, and L. A. Epps, *Inorg. Chem.*, **11**, 2050 (1972).

trans-[Co(acac)₂(SCN)py] leads to the formation of a new species ($t_{1/2} \approx 1$ hr) in addition to the products of geometrical and linkage isomerism. The new species which imparts a emerald green color to the solutions shows a methyl resonance at -2.16 ppm and methine resonance at -5.53 ppm. The *trans*-like spectrum is consistent with a complex of the type *trans*-[Co(acac)₂(SCN)₂]⁻. Both the latter complex and the supposed *cis*-[Co(acac)₂(SCN)py] have not been isolated and further characterized and only have been briefly studied in DMSO solution. Further work on these interesting complexes is warranted. Since the complex *trans*-[Co(acac)₂(SCN)py] shows limited solubility in DMSO and methanol, *i.e.*, $\sim 1.5 \times 10^{-2}$ M and $\sim 0.3 \times 10^{-2}$ M, respectively, initial attempts to form more concentrated solution (about four times) appeared to yield a true solution with rapid subsequent precipitation of a sparingly soluble material which was thought to be *trans*-[Co(acac)₂(NCS)py]. However, from the behavior of the low-concentration solutions it is obvious that the precipitate observed in the more concentrated solution was actually undissolved *trans*-[Co(acac)₂(SCN)py].

The N-bonded *trans* isomer can be isomerized to the *cis* isomer in a few hours by heating in refluxing chloroform.



The reaction does not cleanly yield the *cis* N-bonded isomer but gives a small amount of a Co(II) impurity which can be removed by column chromatography. The speed of geometrical isomerization noted here for the NCS⁻ complex is comparable to that of the closely similar complex¹ of NCO⁻.

Spectral Characterization. The identities of the various solid reaction products and the materials produced *in situ* were established using ir and nmr spectroscopy. The ir spectra are of particular use when considering the linkage isomers *trans*-[Co(acac)₂(NCS)py] and *trans*-[Co(acac)₂(SCN)py]. In most respects, the spectra of these isomers are quite similar and show the same frequencies for the vibrations associated with the acetylacetonate and pyridine ligand.¹¹ On the other hand, by careful examination of the region of the spectrum that shows absorption bands of the coordinated NCS⁻, differences are seen between the isomers. For example, the initial product of the synthetic reaction 1 can be assigned as the thiocyanate, S-bonded, complex since its pellet spectrum shows a sharp medium-intensity band at 2105 cm^{-1} which arises from $\nu(\text{CN})^7$ of the Co^{III}-SCN⁻ complex. The product of the isomerization reaction 2 can be identified as the N-bonded isothiocyanate complex since it shows a strong broad band at 2110 cm^{-1} . The increase in frequency and intensity noted is as expected in going from the S-bonded to the N-bonded isomer.⁸ The assignment of the linkage isomers is corroborated by the observation of a weak band for $\nu(\text{CS})$ at 818 cm^{-1} in the N-bonded form while the S-bonded material does not show this absorption. Unfortunately the $\nu(\text{CS})$ which is expected at $\sim 700 \text{ cm}^{-1}$ in the thiocyanate isomer is obscured by a strong acetylacetonate absorption at 698 cm^{-1} . Finally, the thiocyanate isomer shows two weak bands at 459 and 428 cm^{-1} in the $\delta(\text{NCS})$ region while the isothiocyanate isomer shows only one weak band at 453 cm^{-1} . The complex which forms from *trans*-[Co(acac)₂(NCS)py] via geometrical isomerization (eq 3) is assigned as an isothiocyanate complex, *cis*-[Co(acac)₂(NCS)py], based on the observation of SCN⁻ vibrational absorptions at 2108 cm^{-1} (s, b), 828 cm^{-1} (w), and 435 cm^{-1} (w).

(11) L. J. Boucher and N. G. Paez, *Inorg. Chem.*, **9**, 418 (1970).

Table I. Acetylacetonate Proton Chemical Shifts (ppm)^a for Complexes^b

Assignment	<i>trans</i> -[Co(acac) ₂ (SCN)py]		<i>trans</i> -[Co(acac) ₂ (NCS)py]	<i>cis</i> -[Co(acac) ₂ (NCS)py]	
	CDCl ₃	DMSO- <i>d</i> ₆	CDCl ₃	CDCl ₃	DMSO- <i>d</i> ₆
CH ₃	-2.18	-2.08	-2.22	-2.28	-2.25
				-2.24	-2.20
				-2.19	-2.00
C-H	-5.38	-5.47	-5.44	-1.98	-5.80
				-5.61	-5.58
				-5.38	-5.55

^a Chemical shifts downfield from TMS for CDCl₃ solutions and from DSS for DMSO-*d*₆ solutions. ^b 5% (w/v) solutions, except for *trans*-[Co(acac)₂(NCS)py] which is $\sim 1\%$ (saturated solution).

Table II. Visible-Ultraviolet Absorption Maxima (kK) of Complexes

Complex	Solvent	$\bar{\nu}_{\text{max}}$	
		CDCl ₃	DMSO
<i>trans</i> -[Co(acac) ₂ (SCN)py]	CHCl ₃	~ 17.5 , ^b 25.4 (2.38) ^a	
	Nujol	~ 17.8	
	CH ₃ OH	~ 17.9 , ~ 25.0 , ~ 29.4 , ~ 34.5 , 39.4 (4.28)	
<i>trans</i> -[Co(acac) ₂ (NCS)py]	CHCl ₃	~ 17.9	
	Nujol	~ 18.2	
	CH ₃ OH	18.2, 29.8, ~ 34.8 , 42.9	
<i>cis</i> -[Co(acac) ₂ (NCS)py]	CHCl ₃	17.3 (2.32)	
	Nujol	~ 17.8	
	CH ₃ OH	17.6 (2.60), 31.8 (3.83), ~ 34.5 , 44.3 (4.55)	

^a $\log \epsilon_{\text{max}}$ in parentheses. ^b Shoulder.

Proton magnetic resonance spectroscopy provides the best method of establishing the identity of the geometrical isomer pairs.¹² Chemical shifts and assignments for the spectra of the complexes are given in Table I. The linkage isomers are assigned the *trans* configuration on the basis of the observation of one methyl and one methine resonance with the relative intensity ratio of 6:1, in CDCl₃.³ On the other hand, the low-symmetry *cis* isomer gives the expected multiple methyl, four, and methine, two, resonances in the intensity ratio 3:3:3:3:1:1, in CDCl₃. In agreement with the notion that *cis* effects are small in bis(acetylacetonato)-cobalt(III) complexes,¹² it is seen that the chemical shifts of the linkage isomers are not greatly different. The dimethyl sulfoxide solution spectra show one set of methyl lines, three, and one set of methine lines, two, in the intensity ratio 6:3:3:1:1 for the *cis*-[Co(acac)₂(NCS)py] complex. Unfortunately the *trans*-[Co(acac)₂(NCS)py] isomer is not sufficiently soluble in DMSO to observe a spectrum.

The ultraviolet-visible absorption spectra (Table II) were taken with the complexes in chloroform and methanol solution and in a Nujol mull. The first ligand field band for pseudooctahedral Co(III) $^1A_{1g} \rightarrow ^1T_{1g}$ appears at slightly lower energy for the S-bonded isomers as compared to the N-bonded *trans* isomer, *i.e.*, at 17.5 kK vs. 17.9 kK for chloroform solution. Further there is a low-energy shoulder at ~ 16 kK for the S-bonded isomer. The splitting of the octahedral band into two low-symmetry components is qualitatively in accord with previous spectral data for Co(III) linkage isomers.¹³ The two components of the band have been assigned to the $^1A_{1g} \rightarrow ^1E_g$ transition for the low-energy

(12) L. J. Boucher, E. J. Battis, and N. G. Paez, *J. Inorg. Nucl. Chem.*, **33**, 1373 (1971).

(13) D. A. Buckingham, I. I. Creaser, and A. M. Sargeson, *Inorg. Chem.*, **9**, 655 (1970).

shoulder and $^1A_{1g} \rightarrow ^1A_{2g}$ for the higher energy band. The S-bonded isomer shows the splitting and low-energy shift since the ligand field strength of the ligand is substantially different from the other oxygen and nitrogen donor ligands.¹⁴ Finally a prominent shoulder can be seen at 25.4 kK for the S-bonded isomer which is absent from the N-bonded isomer.

The ultraviolet spectra of the linkage isomers in methanol are quite similar with regard to the frequency of the charge-transfer band: $t_{2g} \rightarrow \pi^*$ at 29.8 kK and the $aca\bar{c} \pi \rightarrow \pi^*$ band at 42.9 kK. A major difference, however, is the presence of an intense band at 39.4 kK ($\log(\epsilon_{max})$ 3.75) in the spectrum of the S-bonded isomer. The band is absent or obscured by the $aca\bar{c}$ bands in the spectrum of the N-bonded form. An analogous band has been previously assigned¹⁵ to a Co(III) \rightarrow SCN⁻ charge transfer for the S-bonded complex $[Co(CN)_5SCN]^{3-}$. The band at 39.4 and 25.4 kK for *trans*- $[Co(acac)_2(SCN)py]$ may have a similar origin.

Comparison of the spectra of the N-bonded geometrical isomers shows the red shift of the charge-transfer and ligand band and the blue shift of the ligand field band normally seen in going from the *cis* to the *trans* isomers for bis(acetylacetonato)cobalt(III) complexes.⁵

Acknowledgment. The authors wish to acknowledge the support of this research by the National Science Foundation via Grant GP-23464.

Registry No. *trans*- $[Co(acac)_2(SCN)py]$, 51933-43-8; $[Co_2(acac)_2(OH)_2]$, 51932-17-3; *trans*- $[Co(acac)_2(NCS)py]$, 51933-44-9; *cis*- $[Co(acac)_2(NCS)py]$, 52019-94-0.

(14) C. K. Jorgensen, *Inorg. Chim. Acta, Rev.*, **2**, 76 (1968).

(15) D. F. Gutterman and H. B. Gray, *J. Amer. Chem. Soc.*, **93**, 3364 (1971).

Contribution from the Corporate Research Laboratories, Owens-Illinois Technical Center, Toledo, Ohio 43651, and the Department of Chemistry, University of South Florida, Tampa, Florida 33620

X-Ray Photoelectron Spectroscopy of Some Aluminosilicates

P. R. Anderson and W. E. Swartz, Jr.*

Received March 26, 1974

AIC40203A

Recently Urch and coworkers¹ have reported that the 2p ionization energy of aluminum having fourfold coordination in microcline, $KAlSi_3O_8$, is about 1.4 eV lower, as determined by X-ray photoelectron spectroscopy, than the 2p ionization energy of aluminum having sixfold coordination in Al_2O_3 . Since the determination of the coordination of aluminum in soda-alumina-silicate glasses and in other non-crystalline materials is an important structural problem,² the ability to determine the coordination by photoelectron spectroscopy of core levels would be a significant accomplishment. The purpose of this study is to investigate the change in binding energy of the aluminum 2p core level as a function of coordination of the aluminum contained in aluminosilicate

* To whom correspondence should be addressed at the University of South Florida.

(1) C. J. Nicholls, D. S. Urch, and A. N. L. Kay, *J. Chem. Soc., Chem. Commun.*, 1198 (1972).

(2) S. Sakka, *Bull. Inst. Chem. Res., Kyoto Univ.*, **49**, 349 (1971).

Table I. Corrected Core Electron Binding energies and Full Widths at Half-Maximum (FWHM) of Elements Contained in Aluminosilicates

Element	Electron level	Mineral	Binding energy (±0.5), eV	FWHM (±0.05), eV	Aluminum coordination
Al	2p	Kyanite	74.9	2.25	6-fold
O	1s	Kyanite	531.5	2.33	6-fold
Si	2p	Kyanite	103.0	1.95	6-fold
Al	2p	Sillimanite	74.9	2.16	50% 6-fold 50% 4-fold
O	1s	Sillimanite	531.5	2.62	50% 6-fold 50% 4-fold
Si	2p	Sillimanite	102.8	1.98	50% 6-fold 50% 4-fold
Al	2p	Mullite	75.0	2.28	41-56% 6-fold 59-44% 4-fold
Al	2s	Mullite	119.6	2.66	41-56% 6-fold 59-44% 4-fold
O	1s	Mullite	531.8	2.79	41-56% 6-fold 59-44% 4-fold
Si	2p	Mullite	103.2	2.41	41-56% 6-fold 59-44% 4-fold

polymorphs. In particular, the 2p binding energies of aluminum contained in sillimanite and mullite, which are refractory minerals having about half the aluminum ions in fourfold coordination and the rest in sixfold coordination, have been determined and are compared to the binding energy of aluminum in kyanite in which the aluminum is only sixfold coordinated.

Experimental Procedure

The elemental electron binding energies were measured with a McPherson ESCA 36 photoelectron spectrometer using unmonochromatized Al K α X-radiation for photoelectron excitation. Compensation for sample charging was made by measuring the binding energies relative to a C 1s energy of 285.0 eV. The carbon is due to residual vacuum pump vapor collecting on the sample surface in the vacuum chamber of the spectrometer.

Kyanite and sillimanite, both Al_2SiO_5 , were selected from relatively massive, high-purity minerals. The mullite sample is a commercial material whose X-ray pattern indicated a major mullite phase and a minor glass phase. All of the aluminum in kyanite is in sixfold coordination,³ whereas the aluminum ions in sillimanite are equally divided among sites having fourfold and sixfold coordination.⁴ The aluminum in mullite is also distributed between fourfold and sixfold coordinations,⁵ with 41-56% of the aluminum having sixfold coordination. The exact percentage of aluminum in sixfold coordination in mullite depends on the ratio of alumina to silica.

In order to obtain relatively uncontaminated surfaces that are truly representative of the bulk aluminosilicates and from which reproducible spectra can be obtained, the brittle crystalline aluminosilicates were fractured under vacuum by a device that has been specifically designed to fracture brittle materials in the vacuum chamber of the McPherson photoelectron spectrometer.⁶ Prior to being mounted in the fracture device, the crystalline materials were cut to the proper shape and were slotted so that the location of the fractured surface could be controlled.

The observed spectral lines were deconvoluted using a computer deconvolution program based on a Simplex pattern search and by assuming a single gaussian distribution. A good fit to the experimental data was observed in all cases.

Results and Discussion

The uncorrected aluminum 2p spectra obtained from the three aluminosilicates are shown in Figure 1, and the corrected electron binding energies along with the full widths at half-maximum obtained by a computer fit of the data

(3) C. W. Burnham, *Z. Kristallogr., Kristallgeometrie, Kristallphys., Kristallchem.*, **118**, 337 (1963).

(4) C. W. Burnham, *Z. Kristallogr., Kristallgeometrie, Kristallphys., Kristallchem.*, **118**, 127 (1963).

(5) R. Sadanaga, M. Tokonami, and Y. Takeuchi, *Acta Crystallogr.*, **15**, 65 (1962).

(6) P. R. Anderson and R. D. Cichy, *J. Electron Spectrosc. Relat. Phenomena*, **2**, 485 (1973).